




Mechanisms involved in the antinociceptive and anti-inflammatory effects of a new triazole derivative: 5-[1-(4-fluorophenyl)-1H-1,2,3-triazol-4-yl]-1H-tetrazole (LQFM-096)

Carina S. Cardoso¹ · Daiany P. B. Silva¹ · Dayane M. Silva¹ · Iziara F. Florentino¹ · James O. Fajemiroye¹ · Lorrane K. S. Moreira¹ · José P. Vasconcelos² · Germán Sanz³ · Boniek G. Vaz³ · Luciano M. Lião⁴ · Danilo da S. Lima⁵ · Fernanda Cristina A. dos Santos⁵ · Ricardo Menegatti² · Elson A. Costa^{1,6} 

Received: 4 December 2019 / Accepted: 24 January 2020
© Springer Nature Switzerland AG 2020

Abstract

The aim of this study was to design, synthesize and evaluate the potential analgesic and anti-inflammatory effects of 5-[1-(4-fluorophenyl)-1H-1,2,3-triazol-4-yl]-1H-tetrazole—(LQFM-096: a new triazole compound) as well as to elucidate its possible mechanisms of action. The oral administration of LQFM-096 (10, 20 or 40 mg/kg) decreased the number of writhing in mice. At the dose of 20 mg/kg, LQFM-096 reduced the licking time at both neurogenic and inflammatory phases of the formalin test. Pretreatment with naloxone (3 mg/kg) and glibenclamide (3 mg/kg) attenuated the antinociceptive effect of LQFM-096 in the first phase of the formalin test. At the dose of 20 mg/kg, LQFM-096 also decreased the licking time in the acidified saline-induced and capsaicin-induced nociception. This effect was blocked by naloxone (3 mg/kg) pretreatment prior to the administration of LQFM-096. In addition, LQFM-096 inhibited hyperalgesia induced by carrageenan and PGE₂. Naloxone (3 mg/kg) attenuated the effect of LQFM-096 through disinhibition of PGE₂-induced hyperalgesia. The anti-inflammatory effect of LQFM-096 was demonstrated in carrageenan-induced oedema or pleurisy as well as CFA-induced arthritis. The hyperalgesia and cellular migration in CFA-induced arthritis were reduced significantly. Altogether, these findings suggest antinociceptive effect of LQFM-096 and implicate the modulation of ASICs/TRPV1 channels by opioid/KATP pathway. The anti-inflammatory effect of LQFM-096 was mediated by a reduction in oedema, leukocytes migration, TNF- α , PGE₂ levels and myeloperoxidase activity.

Keywords Pain · Inflammation · Opioid receptors · ASICs · TRPV1 · TNF- α

Electronic supplementary material The online version of this article (<https://doi.org/10.1007/s10787-020-00685-8>) contains supplementary material, which is available to authorized users.

✉ Elson A. Costa
xico@ufg.br

¹ Department of Pharmacology, ICB, Federal University of Goiás, Campus Samambaia, 314, Goiânia, GO 74001-970, Brazil

² Faculty of Pharmacy, Laboratory of Medicinal Pharmaceutical Chemistry, Federal University of Goiás, Goiânia, GO, Brazil

³ Laboratory of Chromatography and Mass Spectrometry, Chemistry Institute, Federal University of Goiás, Goiânia, GO, Brazil

Introduction

Pain is an unpleasant sensory and emotional experience that is associated with an actual or potential tissue injury (IASP 1994). It alerts the organism to external stimuli or threats

⁴ Chemistry Institute, Federal University of Goiás, Campus Samambaia, Goiânia, GO, Brazil

⁵ Department of Histology, Embryology and Cell Biology, ICB, Federal University of Goiás, Campus Samambaia, 314, Goiânia, GO 74001-970, Brazil

⁶ Laboratório de Farmacologia de Produtos Naturais e Sintéticos – ICB-2, Universidade Federal de Goiás, Sala 216, Goiânia, GO CEP 74001-970, Brazil

and triggers appropriate protective responses (Fein 2011). The noxious stimuli often activate nociceptor fibres to promote signal transduction and transmission to the brain (Gold and Gebhart 2010; Julius and Basbaum 2001).

The transient receptor potential vanilloid 1 (TRPV1) channel and acid-sensing ion channels (ASICs) play important roles in modulating nociceptive signalling. The influx of Na^+ and Ca^{2+} through these channels can trigger membrane depolarization and signal transduction cascades (Deval et al. 2010; Deval and Lingueglia 2015; Wemmie et al. 2013).

Pain development often involves inflammatory mediators such as prostaglandins, bradykinin, cytokines, glutamate, substance P, and calcitonin gene-related peptide. These chemical mediators often sensitize and activate peripheral nociceptors to induce hyperalgesia and allodynia (Ji et al. 2014; Oliveira-Junior et al. 2016).

Opioids and nonsteroidal anti-inflammatory drugs (NSAIDs) are the leading analgesic drugs for the treatment of pain. However, these drugs are associated with side effects such as gastrointestinal, sedation, dependence, and tolerance (Benjamin et al. 2008; Jage 2005; Porreca and Ossipov 2009). Hence, a search for effective and safer analgesics has become a necessity.

Triazole compounds are known for their antibacterial, antifungal, anticancer, and neuroprotective activities (Gupta and Jain 2017; Penthala et al. 2015; Li et al. 2016). This pharmacological profile is associated with the broad interest in medicinal chemistry of triazole compounds and therapeutic applications.

Although some studies have shown anti-inflammatory and antinociceptive activities of triazole derivatives (Hunashal et al. 2014; Joanna et al. 2014; Khanage et al. 2013), the underlying mechanisms of these actions remain unclear. The present study sought to synthesize and investigate the biological activities of LQFM-096 as well as elucidate its possible mechanisms of action.

The LQFM-096 was designed through ring bioisosterism strategy, where pyrazole scaffold present in LQFM-020 (Oliveira et al. 2016) was changed by 1,2,3-triazole scaffold present in LQFM-096 (Fig. 1). The bioisosterism strategy is commonly used in medicinal chemistry drug design (Lima and Barreiro 2005). There are many drugs which showed the 1,2,3-triazole scaffold, i.e. ceftriaxime, rufinamide, and tazobactam, as well as, in many lead compounds (Dheer et al. 2017). Once this scaffold is present on many drugs and lead compounds, it is considered as a privileged structure, in drug designed (Yet 2018). The fluoride scaffold was maintained in order to facilitate solubility in water and biological fluids (Hagmann 2008; Wang et al. 2014). Besides that, the difference in the physical–chemical properties due to scaffold changes between LQFM-020 and LQFM-096 results in expectations of change in the new compound effectiveness in the used experimental models.

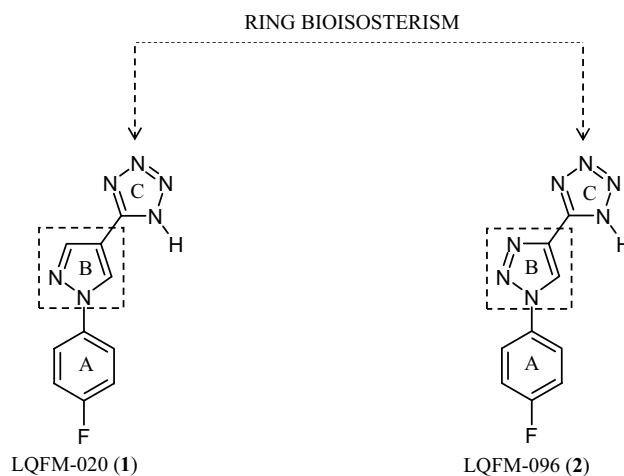


Fig. 1 Structural design of LQFM-096 (2) from LQFM-020 (1) lead compound

Materials and methods

Chemistry

General

The reactions were monitored by TLC using commercially available pre-coated plates (Whatman 60 F254 silica). The developed plates were examined under UV light (254 and 365 nm). The ^1H and ^{13}C -NMR spectra were recorded in the indicated solvent on a Bruker Avance III 500 MHz spectrometer. Chemical shifts were quoted in parts per million downfield of TMS, and the coupling constants were expressed in Hertz. All assignments of the signals of ^1H and ^{13}C NMR spectra are consistent with the chemical structures of the products. Infrared spectra were recorded on a Perkin-Elmer Spectrum Bx-II FT-IR System spectrophotometer instrument as films on KBr discs. Melting points were assessed using a Marte melting point apparatus, and the results were uncorrected. The organic solutions were dried over anhydrous sodium sulphate. The organic solvents were removed under reduced pressure in a rotary evaporator. Mass spectra (MS) were obtained with a microTOF III (Brucker Daltonics Bremen, Germany). To prepare a sample for MS analysis, 1 μg of the sample was diluted in 1 ml of methanol. To perform the analysis in positive mode, 1 μl of formic acid was added to the sample and the resulting solution was infused into the ESI source at a flow rate of 3 $\mu\text{l}/\text{min}$. The ESI(+) source conditions were as follows: nebulizer with nitrogen gas; pressure, 0.4 bar; temperature, 200 $^\circ\text{C}$; capillary voltage, -4 kV, transfer capillary temperature, 200 $^\circ\text{C}$; drying gassed, 4 l/min; end plate offset, -500 V; skimmer, 35 V;

and collision voltage, -1.5 V. Each spectrum was acquired using 2 microscans. The resolving power is $m/\Delta m 50\%$ 16,500.00, where $\Delta m 50\%$ is the peak full width at the half-maximum peak height. Mass spectra were acquired and processed with data analysis software (Bruker Daltonics, Bremen, Germany). Microwave reactions were conducted using a CEM Discovery microwave reactor.

Synthesis of 1-(4-fluorophenyl)-1*H*-1,2,3-triazole-4-carbonitrile (**6**) (Portman 1998)

Distilled water (20 ml) was added to a heated heterogeneous mixture of 1-azido-4-fluorobenzene (**4**) (548 mg, 4 mmol) and 2-chloroacrylonitrile (**5**) (696 mg, 8.00 mmol), and the mixture was heated at 80 °C for 24 h. At the end of the reaction, excess 2-chloroacrylonitrile (**5**) was removed through distillation, cyclohexene (5 ml) was added, and the suspension was stirred for 20 min. The precipitate was filtered under vacuum and dried. The phases were separated and the aqueous layer was extracted with CH_2Cl_2 . The combined organic layers were dried (Na_2SO_4) and concentrated in a vacuum, and the crude product was purified by column chromatography (SiO_2 , $\text{CH}_2\text{Cl}_2/\text{MeOH}=98:2$) to 1-(4-fluorophenyl)-1*H*-1,2,3-triazole-4-carbonitrile (**6**) (661 mg, 88%) as a beige solid with m.p. = 122 – 124 °C and $R_f=0.60$ (hexene/ $\text{AcOEt}=7:3$). IR_{max} (KBr) cm^{-1} : 3132 (ν C-H), 2249 (ν CN), 1515 (ν C=C), and 835 (ν Ar-1,4); $^1\text{H-NMR}$ (500.13 MHz) CDCl_3 (δ): 8.43 (*s*, H-5), 7.74 (*dd*, 9.1; 4.5, H-2'), 7.74 (*dd*, 9.1; 4.5, H-6'), 7.30 (*dd*, 9.1; 7.8, H-3'), 7.30 (*dd*, 9.1; 7.8, H-5'); 2D NMR (HSQC/HMBC-125.76 MHz) CDCl_3/TMS (δ): 163.3 (*d*, 3.7, C-4'), 132.0 (*d*, 3.7, C-1'), 127.6 (*s*, C-5), 123.2 (*d*, 8.7, C-2' and 6'), 122.2 (*s*, C-4), 117.3 (*d*, 23.3, C-3' and 5'), 111.0 (*s*, C-6); $[\text{M} + \text{H}]^+ m/z$ of 189.0543.

Synthesis of 5-(1-(4-fluorophenyl)-1*H*-1,2,3-triazol-4-yl)-1*H*-tetrazole—(LQFM 096) (**2**) (Alterman and Hallberg 2000; Zwaagstra et al. 1997)

Sodium azide (780 mg, 12 mmol) and ammonium chloride (642 mg, 12 mmol) in 10 ml of DMF were added to a heated heterogeneous mixture of 1-(4-fluorophenyl)-1*H*-1,2,3-triazole-4-carbonitrile (**6**) (188 mg, 1 mmol). The resulting mixture was reacted by microwave irradiation (20 W) at 100 °C for 20 min and 1 min of ramp time. The reaction mixture was poured out and acidified to $\text{pH}=5$, and the precipitate formed was filtered off under vacuum and dried. The crude product was crystallized from ($\text{DMF}/\text{AcOH}=9:1$) to 5-(1-(4-fluorophenyl)-1*H*-1,2,3-triazol-4-yl)-1*H*-tetrazole—(LQFM-096) (**2**) (203 mg, 88%) as a beige solid with m.p. = 223 – 226 °C and $R_f=0.58$ ($\text{CH}_2\text{Cl}_2/\text{MeOH}=95:5$). IR_{max} (KBr) cm^{-1} : 3500–3050 (ν N-H), 3029 (ν C-H), 1660 (ν C=C), and 841 (ν Ar-1,4); $^1\text{H-NMR}$ (500.13 MHz) CDCl_3

(δ): 8.99 (*s*, H-5), 8.06 (*dd*, 8.8; 4.7, H-2'), 8.06 (*dd*, 8.8; 4.7, H-6'), 7.50 (*dd*, 8.8; 8.4, H-3'), 7.50 (*dd*, 8.8; 8.4, H-5'); 2D NMR (HSQC/HMBC-125.76 MHz) CDCl_3/TMS (δ): 162.2 (C-4'), 142.4 (C-5'), 133.5 (C-1'), 122.9 (C-2' and 6'), 121.2 (C-4), 120.8 (C-5), 117.3 (C-3' and 5'); $[\text{M} + \text{H}]^+ m/z$ of 232.0708; purity > 98% (supporting information).

Pharmacology

Animals

The experiments were performed using female Swiss albino mice (25–30 g; 7 weeks old) from the Central Animal House of the Federal University of Goiás (UFG). Animals were maintained under controlled temperature (22 ± 2 °C) and luminosity (12 h light/dark cycle) with free access to pellet food and water. The animals were acclimatized for 7 days before beginning the experiments. All of the in vivo studies were previously approved by the Ethics Committee in Animal Experimentation of the Federal University of Goiás (CEUA/UFG, Date of Approval 07/08/2013; Protocol: 017/13). As recommended by the ethics committee, at the end of all the acute tests, the animals were euthanized by cervical dislocation. At the end of the CFA-induced arthritis, the animals were euthanized by decapitation. To prevent bias in the research results, the experimenters were unaware of which animal was receiving a particular treatment.

Drugs and chemicals

LQFM-096 was synthesized at the Laboratory of Medicinal Pharmaceutical Chemistry, Faculty of Pharmacy, UFG as described above. The following drugs were purchased through a pharmaceutical company representative: acetic acid (Synth, Brazil); dimethyl sulphoxide (DMSO) (Sigma Chemical, USA), amiloride (Sigma Chemical, USA), capsaicin (Sigma Chemical, USA), capsazepine (Sigma Chemical, USA), carrageenan (Sigma Chemical, USA), formaldehyde (Synth, Brazil), indomethacin (Prodome, Campinas, SP, Brasil), morphine sulphate (Dimorf[®], Cristalia, SP, Brazil), naloxone hydrochloride (Narcan[®]), and glibenclamide (Sigma-Aldrich, St. Louis, MO, USA). LQFM-096 was dissolved in 10% DMSO in saline, and all other drugs were dissolved in 0.9% saline.

Antinociceptive activity

Acetic acid-induced abdominal writhing Acetic acid-induced abdominal writhing was performed as described by Koster et al. (1959). The animal groups ($n=8$) were treated orally (p.o.) with vehicle (10% DMSO, 10 ml/kg), LQFM-096 (10, 20, or 40 mg/kg) or indomethacin (10 mg/kg, positive control) prior to the administration of the acetic acid

solution (1.2% v/v; 10 ml/kg, intraperitoneally [i.p.]). Each mouse was placed in a big glass cylinder and the number of writhing occurrences was recorded over a 30 min period after the administration of acetic acid. The results were expressed as the mean \pm S.E.M of the number of writhing.

Formalin-induced nociception Formalin-induced nociception was conducted as described by Hanskaar and Hole (1987). The experimental groups of mice ($n = 8$) were treated with vehicle (10% DMSO, 10 ml/kg, p.o.), LQFM-096 (20 mg/kg, p.o.), or indomethacin (10 mg/kg, p.o.—positive control in the second phase) or subcutaneously (s.c.) with morphine (5 mg/kg, positive control in the first phase where direct stimulation of the nociceptors causes neurogenic pain and in the second phase where the release of inflammatory mediators causes inflammatory pain). After an interval of sixty min, 20 μ l of 3% formalin was injected into the plantar surface of the right hind paw prior to the placement of an individual mouse in an acrylic box. A mirror was placed under the box to ensure unhindered observation of the formalin-injected paw for 30 min. Pain reaction time (licking time) was assessed during the following two periods: from 0 to 5 min (first phase) and from 15 to 30 min (second phase). The results were expressed as the mean \pm S.E.M of the licking time in seconds (s).

Antihyperalgesic activity The mice ($n = 10$) were treated with vehicle (10% DMSO, 10 ml/kg, p.o.), indomethacin (10 mg/kg, p.o.) or LQFM-096 (20 mg/kg, p.o.). Sixty min after oral administration, carrageenan (50 μ l) or prostaglandin E₂ (PGE₂) (50 μ l, 100 ng/paw) was injected into the plantar surface of the right hind paw or saline into the contralateral paw. A progressively increasing pressure was applied to the dorsal surface of the inflamed and uninflamed hind paw until a withdrawal reflex was elicited. The nociceptive threshold was evaluated from the difference between the two paws at 1, 2, 3, and 4 h using an analgesimeter (Insight Apparatus EFF-440—Brazil). A 400 g cut-off was set to prevent paw lesions. A baseline (at time 0) was performed for each animal before the treatments (Randall and Selitto 1957; Barbosa et al. 2013). The results were expressed as the mean \pm S.E.M of the response to mechanical stimulus in grams (g).

Study of the antinociceptive mechanism of action *Opioid receptor involvement* The mice ($n = 8$) were pretreated with saline (10 ml/kg, i.p.) or naloxone (3 mg/kg, i.p.). After fifteen min, the animals were treated with vehicle (10% DMSO, 10 ml/kg, p.o.), LQFM-096 (20 mg/kg, p.o.) or morphine (5 mg/kg, s.c.). Sixty min after oral treatment or thirty min after s.c. injection, the mice received formalin (3%, v/v). The licking time was observed and recorded as described in section “[Formalin-induced nociception](#)”. The

results were expressed as the mean \pm S.E.M of the licking time (s).

The involvement of the opioid system in the effect of LQFM-096 on PGE₂-induced hyperalgesia was also investigated. The experimental protocol was performed as described in section “[Antihyperalgesic activity](#)”. The experimental groups of mice ($n = 10$) were pretreated with naloxone (3 mg/kg, i.p.), nonselective opioid receptor antagonist or saline (10 ml/kg) fifteen min prior to oral treatment with the vehicle (10 ml/kg, 10% DMSO), LQFM-096 (20 mg/kg) or morphine (5 mg/kg, s.c.). The results were expressed as the mean \pm S.E.M of the difference between the nociceptive thresholds of the paws (g).

ASIC Involvement To evaluate the involvement of ASICs in the antinociceptive effects of LQFM-096, mice ($n = 8$) were treated with vehicle (10 ml/kg, 10% DMSO, p.o.), LQFM-096 (20 mg/kg, p.o.), amiloride (10 mg/kg, i.p., ASIC inhibitor), or morphine (5 mg/kg, s.c.). Sixty min after oral treatment or thirty min after i.p. or s.c. injection, the mice received a 20 μ l intraplantar injection of acidified saline (2% acetic acid in 0.9% saline, pH 2.0) into the plantar surface of the right hind paw. After the injection of acidified saline, the mice were placed into an acrylic box and the licking time was assessed for 20 min. The results were expressed as the mean \pm S.E.M of the licking time (s) (Meotti et al. 2010; Rios et al. 2013). To verify the involvement of opioid receptors in the effects of LQFM-096 on acid-induced nociception, mice were pretreated with naloxone (3 mg/kg, i.p.) or saline (10 ml/kg, i.p.) fifteen min prior to treatment with vehicle (10 ml/kg, 10% DMSO, p.o.), LQFM-096 (20 mg/kg, p.o.), amiloride (100 mg/kg i.p.), or morphine (5 mg/kg, s.c.).

TRPV Channel Involvement The involvement of TRPV channels in the antinociceptive effects of LQFM-096 was assessed through capsaicin-induced pain. Groups of mice ($n = 8$) were treated with vehicle (10% DMSO, 10 ml/kg, p.o.), LQFM-096 (20 mg/kg, p.o.) or morphine (5 mg/kg s.c.). Sixty min after oral treatment or thirty min after s.c. injection, the mice received a 20 μ l intraplantar injection of capsaicin (1.6 μ g/paw) into the plantar surface of the right hind paw. After the capsaicin injection, the mice were placed into an acrylic box and the licking time was assessed for 7 min. The results were expressed as the mean \pm S.E.M of the licking time (s) (Mohd Sani et al. 2012; Sakurada et al. 1992). To verify the involvement of opioid receptors in the effect of LQFM-096 on capsaicin-induced pain, experimental groups of mice were pretreated with naloxone (3 mg/kg, i.p.) or saline (10 ml/kg, i.p.) fifteen min prior to treatment with vehicle (10 ml/kg, 10% DMSO, p.o.), LQFM-096 (20 mg/kg, p.o.) or morphine (5 mg/kg, s.c.).

K_{ATP} Channel Involvement To investigate the role of K_{ATP} channels in the antinociceptive effect of LQFM-096, mice ($n = 8$) were pretreated with saline (10 ml/kg, i.p.)

or glibenclamide (3 mg/kg, i.p., selective K_{ATP} channel blocker). After fifteen min, the animals were treated with vehicle (10 ml/kg, 10% DMSO, p.o.) or LQFM-096 (20 mg/kg, p.o.). After sixty min, the mice received formalin (3%, v/v) and the licking time was observed as described in section “**Formalin-induced nociception**”. The results were expressed as the mean \pm S.E.M of the licking time (s).

Anti-inflammatory activity

Carrageenan-induced paw oedema This test was performed as described by Passos et al. (2007). Mice ($n=10$) were treated with vehicle (10 ml/kg, 10% DMSO, p.o.), indomethacin (10 mg/kg, p.o.) or LQFM-096 (20 mg/kg, p.o.). After sixty min, the mice received an intraplantar injection of 50 μ l of carrageenan 1% in saline in the right paw. The posterior left paw (control) received an injection of saline solution (0.9%) at the same volume. The paw oedema was evaluated by the differences in the paw volume using a plethysmometer at 1, 2, 3 and 4 h after carrageenan injection. Baseline values were obtained before the treatments. The results were expressed as the mean \pm S.E.M of the difference in the paws in microliters.

Carrageenan-induced pleurisy The pleurisy test was performed according to the method described by Saleh et al. (1999). The experimental groups ($n=8$) were treated with vehicle (10 ml/kg, 10% DMSO, p.o.), dexamethasone (2 mg/kg, p.o.) or LQFM-096 (20 mg/kg, p.o.). Sixty min later, the animals were anaesthetized (2–3% halothane in 100% O_2) prior to the injection of carrageenan (100 μ l of 1% in saline) into the pleural cavity (Moore 2003). Four hours after carrageenan injection, the animals were euthanized and the pleural exudate was collected with 1 ml of heparinized phosphate-buffered saline. An aliquot was used to count the number of total leukocytes using Türk solution in a Neubauer chamber. Differential counting of leukocyte mononuclear and polymorphonuclear cells was also carried out. The results of the total and differential counting were expressed as the mean \pm S.E.M of the absolute number of total cells and each cell type, respectively. The final result was adjusted according to the unit of volume and expressed as the number of leukocytes $\times 10^6$ /ml. An additional aliquot of pleural exudate was used to determine the myeloperoxidase (MPO) activity and quantify the tumour necrosis factor alpha (TNF- α) levels.

Evaluation of MPO activity MPO activity was determined as described previously (Saleh et al. 1999; Sedgwick 1995). The pleural fluid samples (20 μ l) were added to 360 μ l of phosphate buffer containing 0.167 mg/ml of o-dianisidine 2HCl and 0.0005% H_2O_2 at pH 6.0. The enzyme reaction was stopped after 15 min by the addition of 20 μ l of 1%

(w/v) sodium azide. The samples were subsequently centrifuged for 5 min at 300 g. The supernatant (100 μ l) was transferred to a microplate well and the absorbance was monitored at a wavelength of 450 nm. The results were expressed as the mean \pm S.E.M of the enzymatic activity (mU/ml).

Measurement of TNF- α levels After collection of the pleural exudate samples, the TNF- α levels were assessed by enzyme-linked immunosorbent assay (ELISA) using a commercial kit (Ebioscience[®]) according to manufacturer's instructions. Samples were collected 4 h after the induction of pleurisy and centrifuged at 1200 g for 10 min at 4 °C. The supernatant was later separated and stored at -70 °C. The results were expressed as the mean \pm S.E.M of the TNF- α levels in the pleural exudate (pg/ml).

Measurement of prostaglandin E_2 (PGE₂) The concentration of PGE₂ in pleural exudate samples was determined by ELISA using a commercial kit (Cayman Chemical). Samples were collected 4 h after the induction of pleurisy, with PBS containing 10 μ M indomethacin, and then were centrifuged at 1200 g for 4 min at 4 °C, followed by separation and storage (-70 °C) of the supernatant until the assay. Then, the basal PGE₂ values were removed from all of the samples (Florentino et al. 2017). Results were expressed as the mean \pm S.E.M of the PGE₂ levels in the pleural exudate (ng/ml).

CFA-induced arthritis This experiment was performed as described by Chopade and Sayyad (2013). Mice were immunized with an intradermal injection of 50 μ l of Complete Freund's Adjuvant (CFA) (0.5 mg/ml, *Mycobacterium butyricum*) or 50 μ l of saline approximately 1.5 cm distal from the base of the tail. After 7 days, the animals ($n=10$) were subjected to single oral and daily treatment with vehicle (10 ml/kg, 10% DMSO), dexamethasone (2 mg/kg) or LQFM-096 (20 mg/kg) for 14 days. One hour after the first treatment, a monoarthritic reaction was obtained through a second injection of 50 μ l of CFA (0.5 mg/ml, *Mycobacterium butyricum*) or 50 μ l of saline to the right hind paw. The oedema and hyperalgesia were measured 1 h after CFA injection into the paw. These measurements were repeated every 2 days. After measuring the hyperalgesia and oedema on day fourteen, the mice were euthanized by decapitation and the paws were collected to quantify cellular migration through histopathological analysis.

Histopathological analysis The paws were fixed by immersion in Metacarn (proportion: 60% methanol, 30% chloroform, and 10% acetic acid) for 3 h. After fixation, the tissues were dehydrated in ethanol, diaphanized in xylene, and embedded in paraplast (Histosec, Merck, Darmstadt, Germany). The tissues were later sectioned into 5 μ m slices with a manual microtome (Leica RM2155,

Nussloch, Germany). The sections were stained with haematoxylin–eosin (HE) for the quantification of cell infiltration. Thirty photomicrograph fields under a 40× objective were obtained for analysis (6 fields/animal; n=5 animals/group). The absolute number of mononuclear and polymorphonuclear cells *per* photomicrograph field was obtained from the photomicrographs. An A1 light microscope (Carl Zeiss Microscopy, Gottingen, Germany) was used for the analysis and the images were scanned using the ZEN2012-1.1.2.0 software (Zeiss) and Image-Pro Plus version 6.1 for Windows (Media Cybernetics Inc., Silver Spring, MD, USA).

Statistical analysis

The data were statistically analysed by a one-way ANOVA followed by Newman–Keul's post hoc test or by two-way ANOVA followed by Bonferroni's post hoc test (Sokal and Rohlf 1981). All statistical analyses were carried out using GraphPad Prism version 5.00 and the data were expressed as the mean ± S.E.M. Values of $P \leq 0.05$ were considered significant.

Results

Synthesis of 5-(1-(4-fluorophenyl)-1H-1,2,3-triazol-4-yl)-1H-tetrazole—(LQFM-096)

As illustrated in Fig. 2, the synthetic route began with 1-azido-4-fluorobenzene (**4**) and proceeded through the diazotization of 4-fluoroaniline (**3**) in a quantitative yield, which was used without purification in the next step (L'abbé et al. 1990). In turn, 1,3-bipolar cycloadditions were carried out between 1-azido-4-fluorobenzene (**4**) and 2-chloroacrylonitrile (**5**) in water to offer 1-(4-fluorophenyl)-1H-1,2,3-triazole-4-carbonitrile (**6**) at 88% yield (Portman 1998). 5-(1-(4-fluorophenyl)-1H-1,2,3-triazol-4-yl)-1H-tetrazole—(LQFM-096) was synthesized through another 1,3-bipolar

cycloaddition between 1-(4-fluorophenyl)-1H-1,2,3-triazole-4-carbonitrile (**6**) and NaN_3 , using NH_4Cl as the catalyst in DMF under microwave irradiation for 20 min with an 88% yield (Alterman and Hallberg 2000; Zwaagstra et al. 1997). When we used the same experimental conditions, but with conventional heat, (**2**) was obtained after 72 h at 88% yield (Zwaagstra et al. 1997). The synthetic route used a green chemistry approach that had an atom economy greater than 80% in each step; a green solvent, *i.e.*, water; and a microwave-assisted organic synthesis (MAOS) (Roschangar, Sheldon, and Senanayake 2015; Trost 1991). LQFM-096 was obtained at 77% overall yield after three steps.

Pharmacology

Antinociceptive activity of LQFM-096

Acetic acid-induced abdominal writhing As shown in Fig. 3, oral treatment with LQFM-096 (10, 20, or 40 mg/kg) decreased the number of writhes in a dose-dependent manner [30.8% ($P < 0.001$), 42.3% ($P < 0.001$), and 51.3% ($P < 0.001$), respectively] when compared to the control group (95.1 ± 5.0). Indomethacin (positive control) decreased the number of writhes by 40% ($P < 0.001$).

Formalin-induced nociception In the formalin test, oral treatment with LQFM-096 (20 mg/kg) reduced the formalin-induced paw licking time in both the neurogenic and inflammatory phases compared to the control group (67.6 ± 4.7 s in the 1st phase and 221.4 ± 19.8 s in the 2nd phase). LQFM-096 reduced the licking time by 56.5% ($P < 0.01$) and 43.1% ($P < 0.01$) in the first and second phases, respectively. Indomethacin decreased the licking time in the second phase (55%, $P < 0.001$), while morphine decreased this parameter in the first (90.4%, $P < 0.001$) and second (95.7%, $P < 0.001$) phases (Fig. 4).

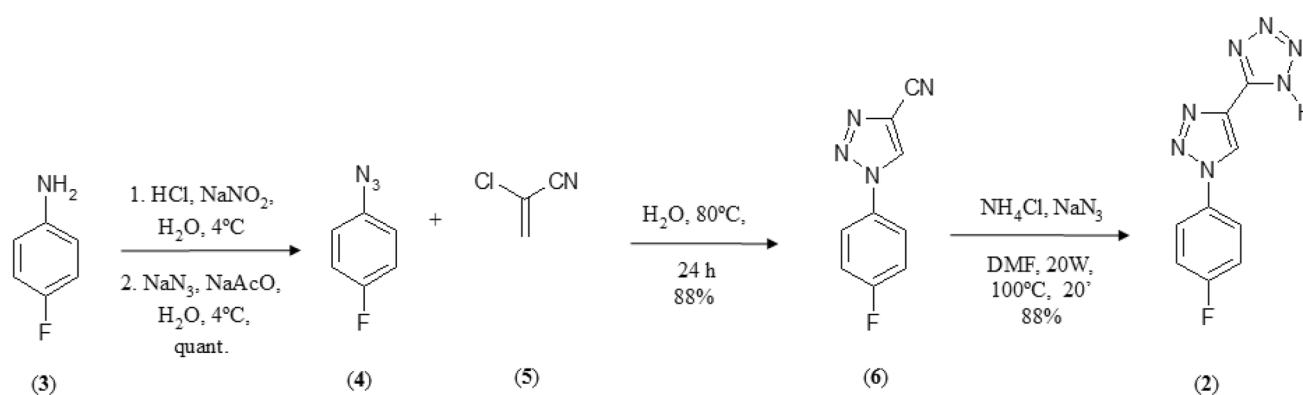


Fig. 2 Synthetic route for the preparation of 5-(1-(4-fluorophenyl)-1H-1,2,3-triazol-4-yl)-1H-tetrazole (**2**) (LQFM-096)

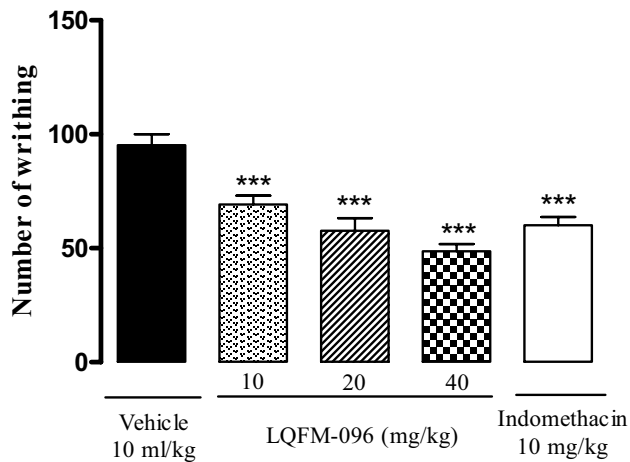


Fig. 3 Antinociceptive effect of LQFM-096 (10, 20, 40 mg/kg, p.o.) in the acetic acid-induced abdominal writhing test, in mice ($n=8$) for 30 min. Indomethacin was used as a positive control. The vertical bars represent the mean \pm S.E.M of the number of writhing for 30 min. *** $P \leq 0.001$ compared to the control group, according to one-way ANOVA followed by the Newman Keuls' post-test

Antihyperalgesic effect of LQFM-096 As shown in Fig. 5a, oral treatment with LQFM-096 (20 mg/kg) or indomethacin (10 mg/kg) reduced the nociceptive threshold between the uninflamed and inflamed paws in response to mechanical stimuli throughout the test. LQFM-096 reduced the nociceptive threshold between the paws by 23% ($P < 0.001$), 28% ($P < 0.001$), 30% ($P < 0.001$), and 33% ($P < 0.001$) in the 1st, 2nd, 3rd and 4th hour of the test, respectively, compared to the control group (152 ± 3.3 g in the 1st hour, 156 ± 2.7 g in the 2nd hour, 154 ± 2.7 g in the 3rd hour, and 150 ± 3.0 g

in the 4th hour). Indomethacin (positive control) also reduced the nociceptive threshold between the paws. In the PGE₂-induced hyperalgesia, LQFM-096 reduced the nociceptive threshold between the paws by 86.6% ($P < 0.001$) in the 1st hour, 75.6% ($P < 0.001$) in the 2nd hour, 80% ($P < 0.001$) in the 3rd hour and 80.8% ($P < 0.001$) in the 4th hour compared to the control group (149.0 ± 18.6 g, 155.1 ± 6.7 g, 205.9 ± 5.7 g, and 206.9 ± 8.5 g in the 1st, 2nd, 3rd and 4th hour of the test, respectively). Indomethacin did not inhibit the hyperalgesia ($P > 0.05$; Fig. 5b).

Antinociceptive mechanism of LQFM-096 Opioid receptor involvement Administration of the nonselective opioid receptor antagonist naloxone (3 mg/kg, i.p.) did not, per se, affect formalin-induced nociception. This compound only antagonized the antinociceptive effect of LQFM-096 (20 mg/kg p.o.) in the first phase of the formalin test ($P > 0.05$) and reversed the antinociceptive effect of morphine in both phases (Fig. 6). In the PGE₂-induced hyperalgesia, naloxone (3 mg/kg, i.p.) attenuated the antihyperalgesic effect of LQFM-096 (20 mg/kg, p.o.) or morphine (5 mg/kg, s.c.) ($P > 0.05$) (Table 1).

ASIC Involvement Oral treatment with LQFM-096 (20 mg/kg) elicited a significant antinociceptive effect with a 53% reduction in the licking time compared to the control group (229 ± 9.4 s; $P < 0.001$; Fig. 7a). Amiloride (positive control) decreased the licking time by 85.1% ($P < 0.001$; Fig. 8a). Unlike amiloride, the antinociceptive effect of LQFM-096 ($P > 0.05$) was blocked by pretreatment with naloxone (3 mg/kg, i.p.).

TRPV Channel Involvement As shown in Fig. 7b, capsaicin-induced pain was reduced in mice treated with

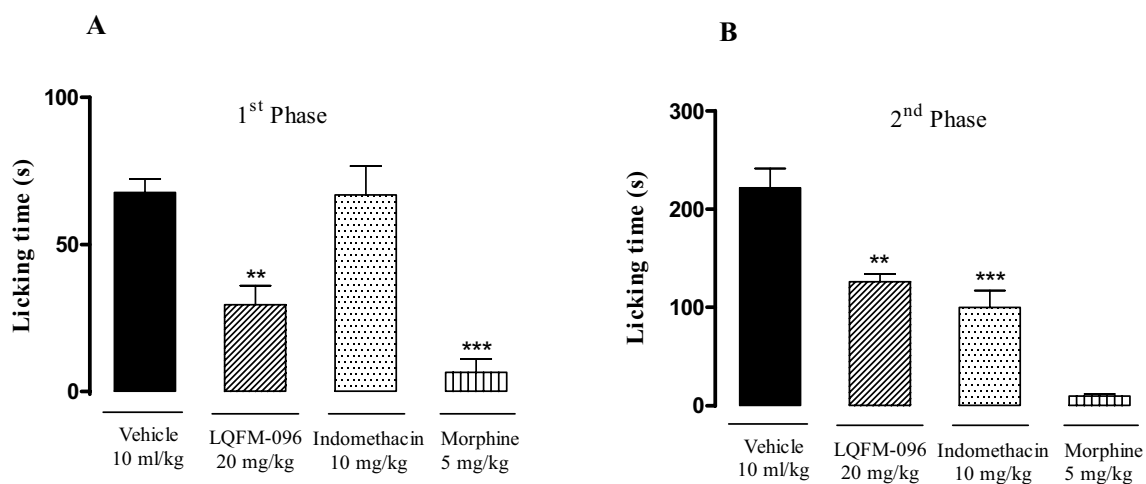


Fig. 4 Antinociceptive effect of LQFM-096 (20 mg/kg, p.o.) in the first phase (a) and second phase (b) of formalin test, in mice ($n=8$). Indomethacin and morphine were used as positive controls, during the first (0–5 min) and second phase (15–30 min). Vertical bars represent

mean \pm S.E.M of licking time (s). ** $P \leq 0.01$ and *** $P \leq 0.001$ compared to control group, according to one-way ANOVA followed by Newman Keuls' post-test

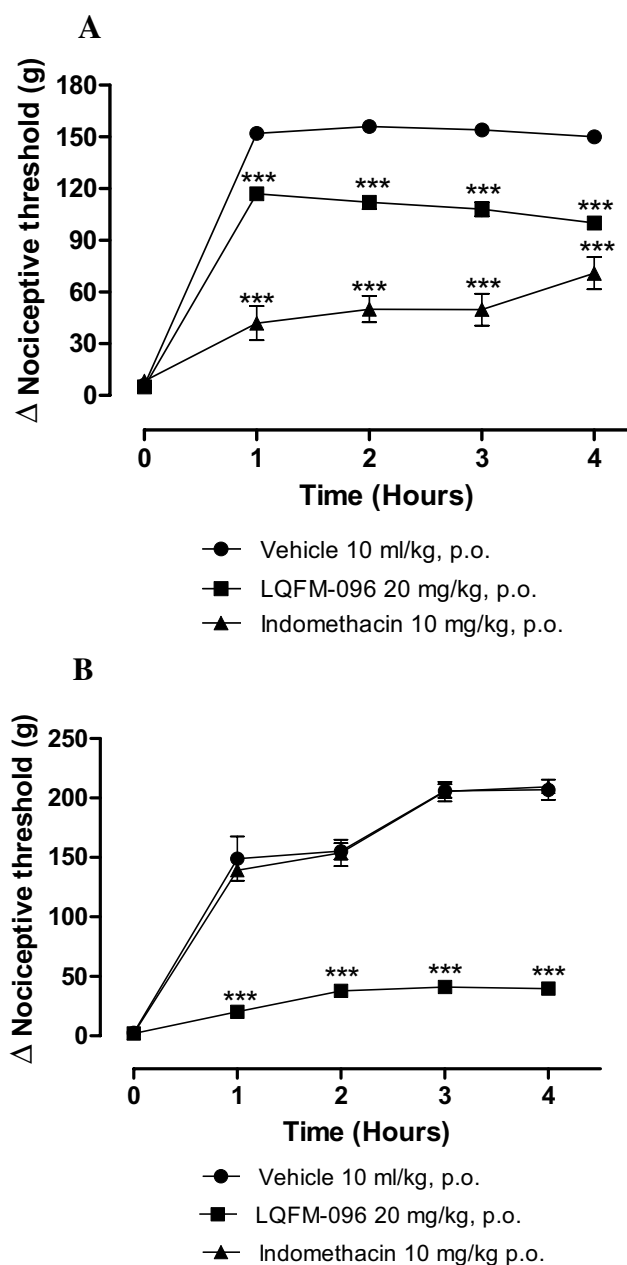


Fig. 5 Effect of LQFM-096 (20 mg/kg, p.o.) on hyperalgesia induced by carrageenan (a) and PGE₂ (b), in mice (n=10). Indomethacin (10 mg/kg, p.o.) was used as positive control. The values were expressed as mean ± S.E.M of the difference of nociceptive threshold between the non-inflamed and inflamed paw of animals in response to mechanical stimulus (g). *** $P \leq 0.001$, compared to control group, according to two-way ANOVA followed by Bonferroni's post-test

LQFM-096 (20 mg/kg, p.o.). LQFM-096 induced a 33.8% inhibition in the licking time compared to the control group (59.4 ± 2.1 s; $P < 0.001$). Pretreatment with naloxone (3 mg/kg, i.p.) reversed the antinociceptive effect of LQFM-096.

K_{ATP} Channel Involvement The role of K_{ATP} channels was evaluated in the formalin test through the administration of

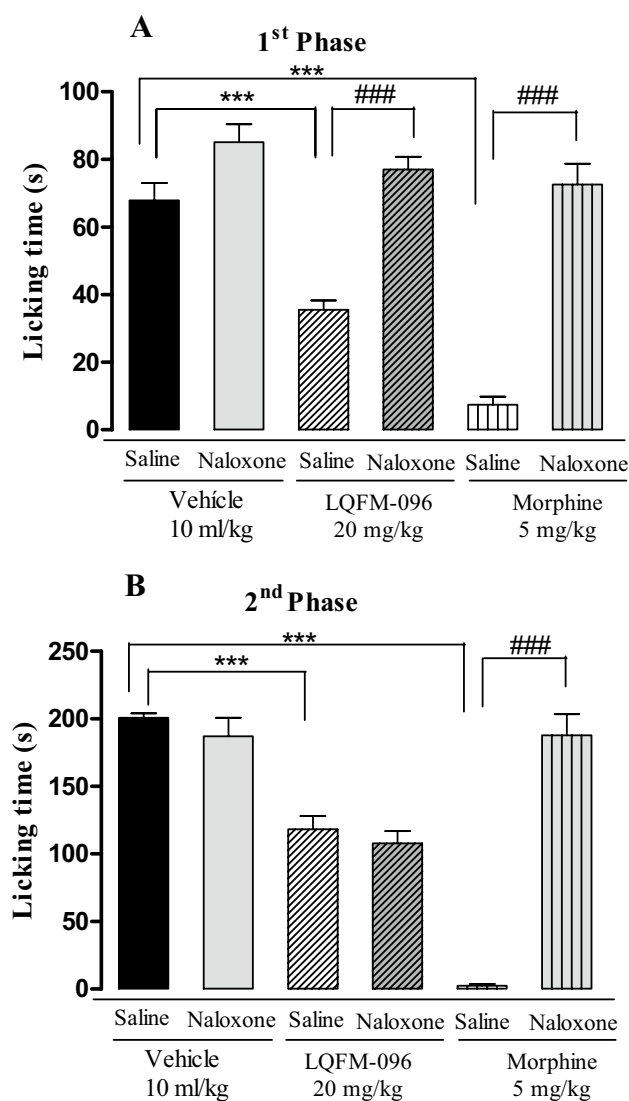


Fig. 6 Effect of pre-treatment with saline (10 ml/kg i.p.) or the non-selective opioid receptor antagonist naloxone (3 mg/kg i.p.) on the LQFM-096 (20 mg/kg p.o.) antinociceptive effect in the first phase (a) and second phase (b) of the formalin test, in mice (n=8). Vertical bars represent mean ± S.E.M of licking time (s). *** $P \leq 0.001$, compared to vehicle that received saline or ### $P \leq 0.001$ compared to group treated that received saline, according to one-way ANOVA followed by post hoc Newman Keuls'test

glibenclamide (3 mg/kg, i.p.—ATP-sensitive K⁺ channel inhibitor). Glibenclamide did not change the effect of formalin-induced nociception per se. Unlike the second phase of the formalin test, the antinociceptive effect of LQFM-096 (20 mg/kg p.o.) was only blocked by glibenclamide ($P > 0.05$) in the first phase, as is shown in Fig. 8.

Anti-inflammatory activity

Carrageenan-induced paw oedema Oral treatment with LQFM-096 (20 mg/kg) reduced the volume of paw oedema

Table 1 Involvement of opioid receptors in the anti-hyperalgesic effect of LQFM-096 (2) in PGE₂-induced hyperalgesia test, in mice (n = 10)

	Difference between the nociceptive thresholds of paws (g) (Mean ± SEM)	
	Saline	Naloxone
1st hour		
Vehicle 10 ml/kg, p.o.	180.6 ± 12.8	136.5 ± 11.2
LQFM-096 20 mg/kg, p.o.	14.7 ± 2.6***	103.0 ± 10.2###
Morphine 5 mg/kg, s.c.	5.7 ± 1.6***	151.2 ± 13.4###
2nd hour		
Vehicle 10 ml/kg, p.o.	196.3 ± 11.7	189.4 ± 8.8
LQFM-096 20 mg/kg, p.o.	13.4 ± 2.1***	141.8 ± 12.6###
Morphine 5 mg/kg, s.c.	9.4 ± 2.03***	160.1 ± 14.8###
3th hour		
Vehicle 10 ml/kg, p.o.	184.6 ± 11.8	185.2 ± 12.2
LQFM-096 20 mg/kg, p.o.	12.7 ± 1.8***	173.9 ± 15.8###
Morphine 5 mg/kg, s.c.	13.8 ± 5.0***	189 ± 17.3###
4th hour		
Vehicle 10 ml/kg, p.o.	198.6 ± 12.0	206.0 ± 8.1
LQFM-096 20 mg/kg, p.o.	17.2 ± 1.8***	176.1 ± 13.4###
Morphine 5 mg/kg, s.c.	28.4 ± 3.9***	183.3 ± 13.1###

Values are expressed as mean ± S.E.M. of the difference of nociceptive threshold between the non-inflamed and inflamed paw of animals in response to mechanical stimulus (g). *** $P \leq 0.001$, compared to vehicle that received saline or ### $P \leq 0.001$ compared to group treated that received saline, according to two-way ANOVA followed by Bonferroni's post-test

by 19.6% ($P < 0.001$), 40.1% ($P < 0.001$), 40.5% ($P < 0.001$) and 36.2% ($P < 0.001$) in the 1st, 2nd, 3rd and 4th hour, respectively, compared to the control group (118.9 ± 4.8 µl, 131.4 ± 8.3 µl, 123.3 ± 9.0 µl and 119.0 ± 5.0 µl in the 1st, 2nd, 3rd and 4th hour, respectively). Indomethacin (10 mg/kg, p.o.) reduced oedema by 39.2%, 49.3%, 47.3% and 50.4% in the 1st, 2nd, 3rd and 4th hour, respectively ($P < 0.001$; Fig. 9a).

Carrageenan-induced pleurisy In the carrageenan-induced pleurisy test, LQFM-096 (20 mg/kg, p.o.) reduced the number of total leukocytes that migrated to the pleural cavity by 41% ($P < 0.001$) compared to the control group (9.5 ± 0.3 × 10⁶ leukocytes/ml). Dexamethasone (2 mg/kg, p.o., positive control) reduced cell migration by 67.6%. The differential count showed that the reduction in cellular migration was due to a decrease in the number of polymorphonuclear cells. The data in Table 2 showed that LQFM-096 or dexamethasone reduced the number of polymorphonuclear cells to 2.5 ± 0.2 and 0.6 ± 0.2 polymorphonuclear cells/ml × 10⁶, respectively, compared to the control group (6.5 ± 0.3 polymorphonuclear cells/ml × 10⁶).

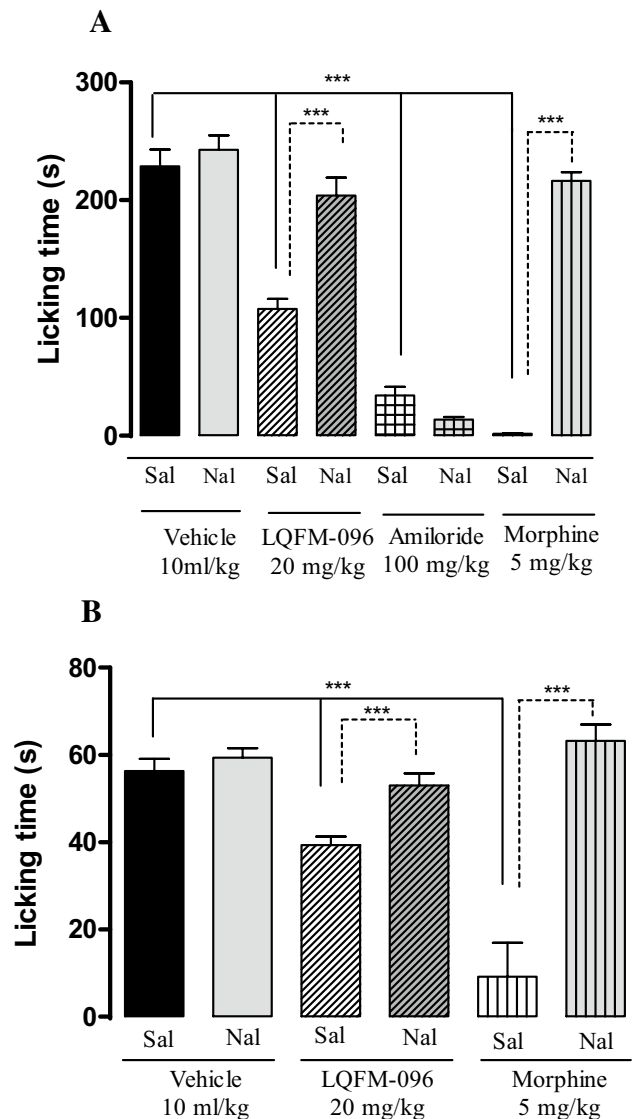


Fig. 7 Effect of pre-treatment with saline (10 ml/kg i.p.) or the non-selective opioid receptor antagonist naloxone (3 mg/kg i.p.) on the LQFM-096 (20 mg/kg p.o.) antinociceptive effect in acidified saline test (a) and capsaicin-induced nociception test (b), in mice (n = 8). Amiloride and morphine were used as positive controls. Vertical bars represent mean ± S.E.M of licking time (s). *** $P \leq 0.001$ compared to control group or naloxone treated group, according to one-way ANOVA followed by post hoc Newman-Keuls' test

Evaluation of MPO activity Oral treatment with LQFM-096 (20 mg/kg) inhibited MPO activity by 39.3% ($P < 0.01$) compared with the control group (74.8 ± 9.1 mU/ml). Similarly, treatment with dexamethasone (2 mg/kg, p.o., positive control) also reduced the activity of this enzyme by 76.7% ($P < 0.001$; Table 2).

Measurement of TNF-α levels Oral administration of LQFM-096 (20 mg/kg) reduced the TNF-α levels by 24.4% ($P < 0.05$) compared with the control group (107.9 ± 8.7 pg/

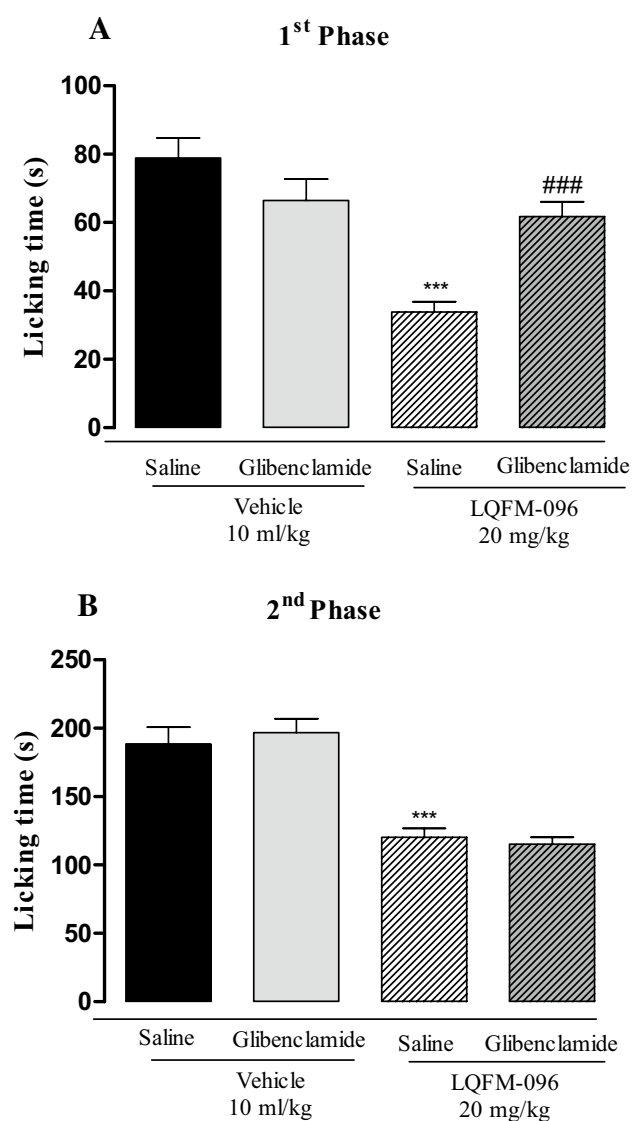


Fig. 8 Effect of pre-treatment with saline (10 ml/kg i.p.) or the selective K_{ATP}^+ antagonist glibenclamide (3 mg/kg i.p.) on the LQFM-096 (20 mg/kg p.o.) antinociceptive effect in the first phase (a) and second phase (b) of the formalin test, in mice ($n=8$). Vertical bars represent mean \pm S.E.M of pain reaction time (s). *** $P \leq 0.001$, compared to vehicle that received saline or ### $P \leq 0.001$ compared to group treated that received saline, according to one-way ANOVA followed by Newman Keuls' post-test

ml). Dexamethasone (2 mg/kg, p.o., positive control) also reduced the TNF- α levels by 88.7% ($P < 0.001$; Table 2).

Measurement of PGE₂ levels PGE₂, a major product of the enzymatic reaction catalyzed by COX-2 in inflammatory process, was also analyzed. Compared with the control group (21.8 ± 0.2 ng/ml), treatment with LQFM-096 20 mg/kg showed significant reduction of the PGE₂ levels by 16.5%. Dexamethasone showed the expected profile and reduced the PGE₂ levels by 22% (Table 2).

CFA-induced arthritis The CFA-induced hyperalgesia in this model was reduced by LQFM-096 (20 mg/kg, p.o.) or dexamethasone (2 mg/kg, p.o.) in all the assessments (Fig. 9b). Although dexamethasone reduced the oedema in all the evaluations, treatment with LQFM-096 did not inhibit oedema formation (Fig. 9c).

Histopathological analysis The histopathological analysis showed an increase in cell infiltration, mainly by polymorphonuclear cells, in the paw dermis of animals treated with vehicle compared with the uninjured group. Administration of LQFM-096 or dexamethasone reduced the infiltration of polymorphonuclear cells (Figs. 9d, 10).

Discussion

The design, synthesis, and pharmacological evaluation of a new triazole derivative, LQFM-096, were reported in this study. This compound elicited antinociceptive effects that were mediated by the opioid/KATP and ASIC/TRPV1 pathways. Our findings also demonstrated the anti-inflammatory effects of this compound as well as reduced cell migration, MPO activity and TNF- α levels. The doses of LQFM-096 in this study were extrapolated from previous experiments with LQFM-020 (LQFM-096 precursor) (Oliveira et al. 2016).

To investigate the antinociceptive effects of LQFM-096, the acetic-acid-induced abdominal writhing test was performed. In general, acetic acid induces nociception through the release of mediators (such as bradykinin, pro-inflammatory cytokines, serotonin, histamine, and prostaglandins) and the activation of ASICs, TRPV1, and glutamate receptors (Costa et al. 2013; Gregory et al. 2013). The LQFM-096-induced reduction in the number of writhes suggests antinociceptive activity. Since LQFM-096 treatment at 40 mg/kg (highest dose) did not induce a significant change in the barbiturate sleep and open field tests, the antinociceptive effects of this compound are unlikely to compromise motor activity or be associated with sedation (Supplementary Material). In subsequent evaluations, the intermediate dose of LQFM-096 with a margin of safety was adopted to reduce the number of experimental animals.

The formalin test was also employed to confirm the antinociceptive effects of LQFM-096. Neurogenic and inflammatory pain can be evaluated in the first and second phases of this test, respectively (Hanskaar and Hole 1987; Shibata et al. 1989). The reduction in the licking time in both phases of this test confirmed the antinociceptive effects of LQFM-096. The result obtained with LQFM-096 against neurogenic pain shows larger effectiveness when compared with the result obtained with LQFM-020 (Oliveira et al. 2016) in the same experimental model, guiding this research to

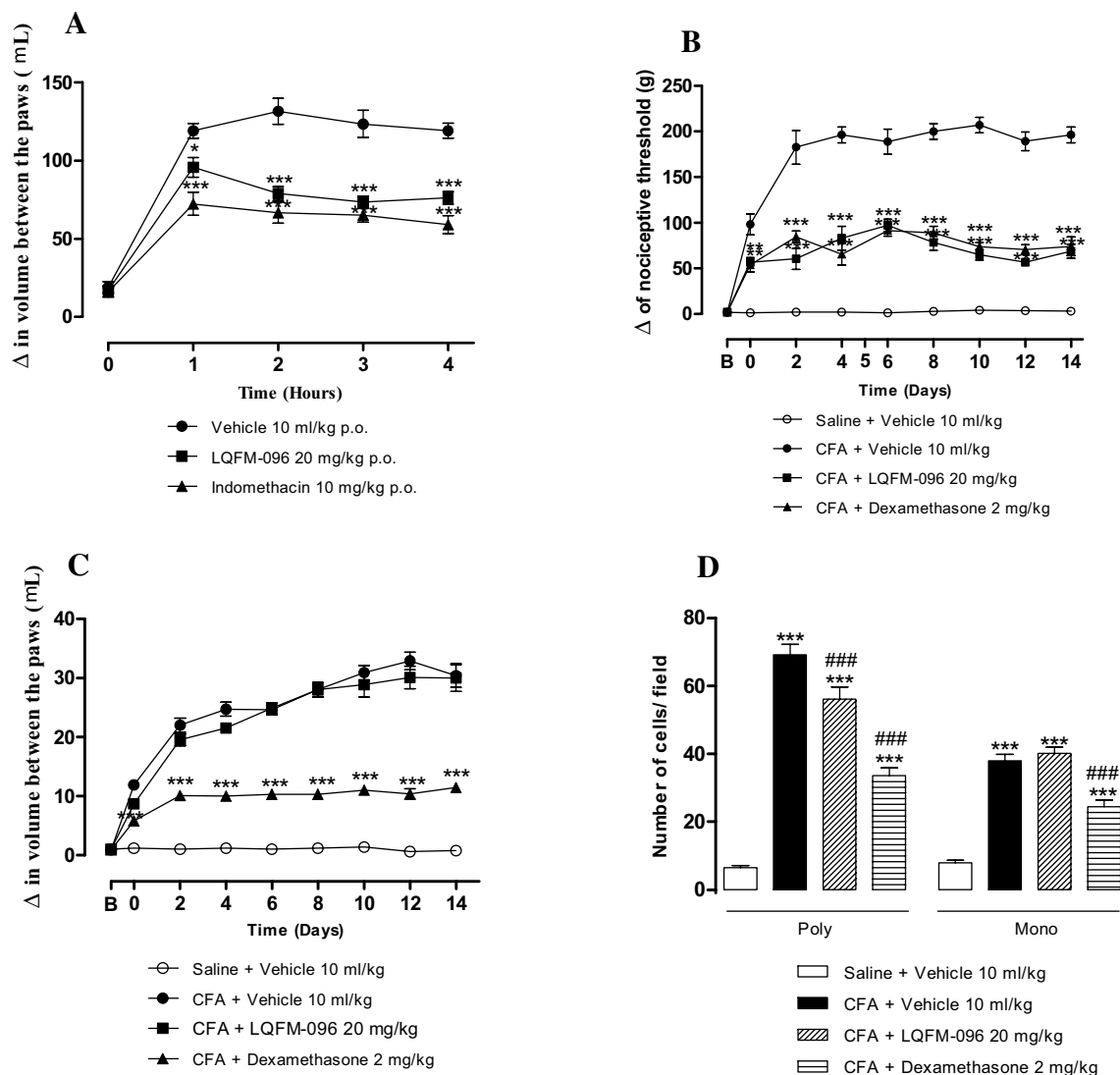


Fig. 9 Effect of LQFM-096 (20 mg/kg, p.o.) on acute and chronic inflammation, in mice. The graphs show the effect of LQFM-096 (20 mg/kg, p.o.) on **a** carrageenan-induced paw oedema test (acute inflammation), **b** CFA-induced hyperalgesia, **c** CFA-induced oedema and **d** cell quantification obtained from histopathological analysis of paw of animals submitted to the CFA-induced arthritis test. Indomethacin (10 mg/kg, p.o.) and dexamethasone (2 mg/kg, p.o.) were used as positive control. The graphics in line represent the mean \pm S.E.M of the difference in volume between the paws, in microliters or the difference of nociceptive threshold between the

non-inflamed and inflamed paw of animals in response to mechanical stimulus (g). (n=10). The vertical bars represent the mean \pm S.E.M of mononuclear and polymorphonuclear leukocytes number that migrates to the paw dermis from thirty photomicrographs fields per group. *** $P \leq 0.001$, compared to control group not injured and ### $P \leq 0.001$, compared to control group injured, according to one-way ANOVA followed by Newman-Keuls' post-test or according to two-way ANOVA followed by Bonferroni's post-test. *Mono* mononuclear, *Poly* polymorphonuclear

elucidating the possible mechanisms of action involved in this antinociceptive effect.

The elucidation of the mechanisms underlying the antinociceptive activities of LQFM-096 was proposed to further the pharmacological characterization of this new compound. To verify whether LQFM-096-induced antinociception is associated with anti-inflammatory activity, carrageenan- or prostaglandin-induced hyperalgesia were carried out. Inflammation often induces hyperalgesia through the sensitization

of the primary nociceptive fibres by inflammatory mediators (Anseloni et al. 2003; Chandy and Moore 1998).

According to Tsuchida et al. (2015), carrageenan injection into an animal's paw increased prostaglandin levels, which in turn sensitize the nociceptive fibres. PGE₂ injection activates the EP1 and EP4 receptors in the nociceptive fibres. These receptors often induce intracellular signal cascades that culminate in hyperalgesia (Kawabata 2001). The experimental data showed that LQFM-096 inhibited

Table 2 Anti-inflammatory activity of LQFM-096 in carrageenan-induced pleurisy test, in mice (n=8)

Inflammatory Parameters	Vehicle 10 ml/kg, p.o.	LQFM-096 20 mg/kg, p.o.	Dexamethasone 2 mg/kg, p.o.
Total leukocytes $\times 10^6/\text{ml}$	9.5 \pm 0.3	5.6 \pm 0.6 ***	3.1 \pm 0.2***
Polymorphonuclears cells $\times 10^6/\text{ml}$	6.5 \pm 0.3	2.5 \pm 0.2***	0.6 \pm 0.2***
Mononuclears cells $\times 10^6/\text{ml}$	3.0 \pm 0.3	3.1 \pm 0.2	2.9 \pm 0.4
MPO activity (mU/ml)	74.8 \pm 9.1	45.4 \pm 7.6**	17.4 \pm 2.6***
TNF- α levels (pg/ml)	107.9 \pm 8.7	81.6 \pm 7.0*	12.29 \pm 3.1***
PGE ₂ levels (ng/ml)	21.8 \pm 0.2	18.2 \pm 1.1***	16.9 \pm 0.7***

Values are expressed as mean \pm S.E.M. of total number of leukocytes $\times 10^6/\text{ml}$, number of polymorphonuclears cells $\times 10^6/\text{ml}$ and number of mononuclears cells $\times 10^6/\text{ml}$ migrated into the pleural cavity, as well as the MPO activity (mU/ml), TNF- α levels (pg/ml) and PGE₂ levels (ng/ml) in the pleural exudate. * $P \leq 0.05$, ** $P \leq 0.01$ and *** $P \leq 0.001$, according one-way ANOVA followed by Student–Newman–Keuls' test

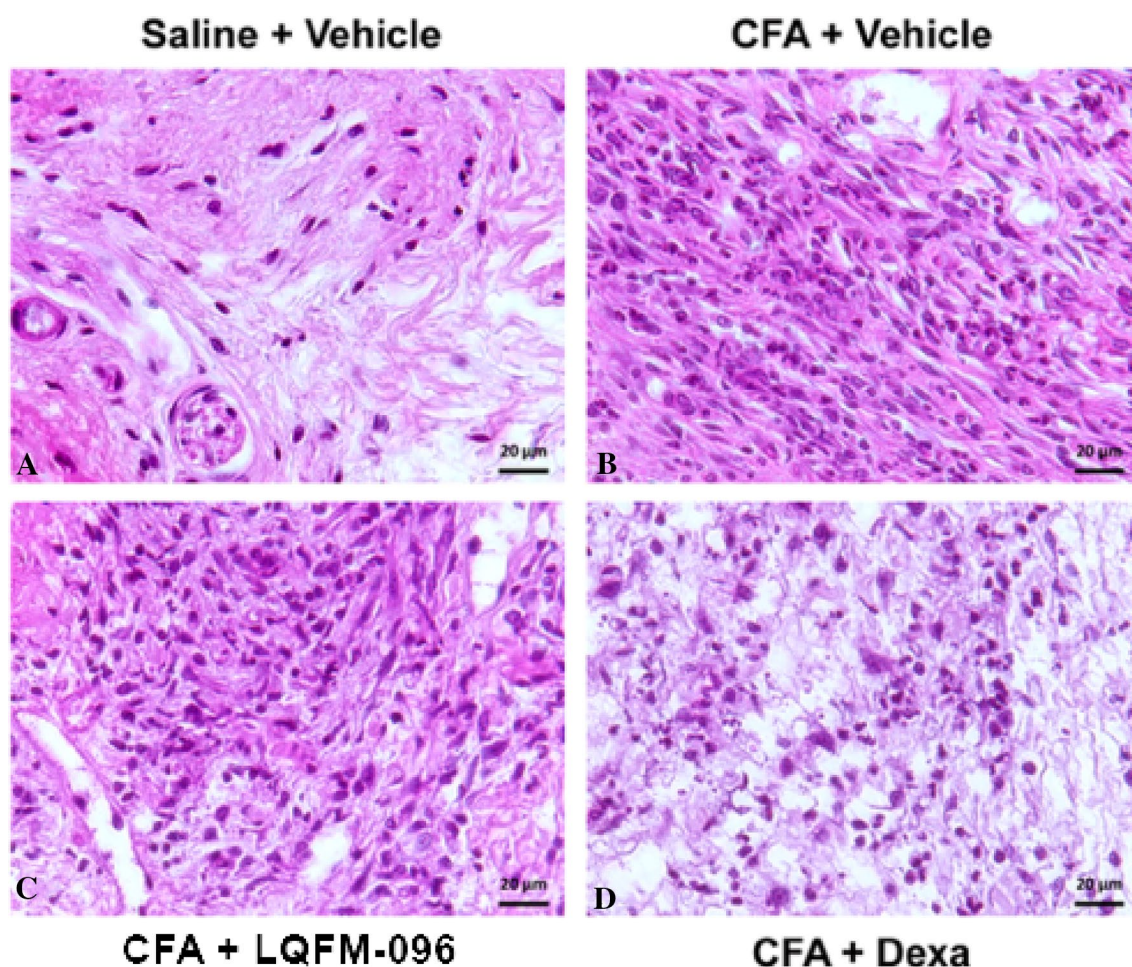


Fig. 10 Histopathology of the paw dermis of the control group not injured (**a**), control group injured (**b**) and groups treated with LQFM-096 (**c**) and dexamethasone (**d**). The absence of cellular infiltration was observed in the group Saline+Vehicle (**a**). The group

CFA+Vehicle showed prominent inflammatory cells infiltration (**b**), while LQFM-096 and dexamethasone were reduced this infiltration (**c**, **d**). The photomicrographs were taken with 40 \times objective (Staining: hematoxylin–eosin). Scale bar of histology: 20 μm

carrageenan- or PGE₂-induced hyperalgesia. Hence, the antinociceptive effects of LQFM-096 suggest the involvement of mechanisms that are independent of inhibitory actions on PGE₂ synthesis.

Opioid receptors play important roles in analgesia by inhibiting adenylate cyclase, reducing cAMP, and releasing neurotransmitters, among others (Sehgal et al. 2011). In this manner, we assessed the participation of opioid receptors in the antinociceptive effects of LQFM-096. In PGE₂-induced hyperalgesia, the effect of LQFM-096 was blocked by naloxone. Additional characterization of this effect was performed in the formalin test with naloxone pretreatment. The results showed that naloxone only blocked the antinociceptive effects of LQFM-096 in the first phase of the formalin test. Thus, the antinociceptive effects appear to be partially mediated by opioid receptors. Opioid receptor activation promotes the opening of K⁺ channels, K⁺ efflux and cellular hyperpolarization (Campbell and Welch 2001). Thus, we investigated the participation of the ATP-sensitive K⁺ channel by using glibenclamide (ATP-sensitive K⁺ channel inhibitor). The antinociceptive effect of LQFM-096 in the first phase of the formalin test was attenuated by pretreatment with glibenclamide. These results confirm the involvement of the opioid/K_{ATP}⁺ pathway in the antinociceptive effect of LQFM-096, which is consistent with that of PILAB 8 (triazole compound) as reported by Montes et al. (2017). Thus, 1,3,5-trisubstituted 1,2,4-triazoles have shown potent and selective δ opioid receptor binding (Peng et al. 2009).

The ASICs and TRPV1 ion channels are involved in the genesis of pain, particularly in inflammatory conditions with tissue acidosis (Baggio et al. 2012; Deval et al. 2010; Ma and Quirion 2007; Mickle et al. 2016). Hence, these channels are important pharmacological targets for the development of new analgesic drugs. Our findings showed that LQFM-096 attenuated the nociception induced by acidified saline (an agonist of ASICs) or capsaicin (an agonist of TRPV1). These results suggest that LQFM-096 can modulate ASICs and TRPV1 ion channels.

A study carried out by Cai et al. (2014) showed that morphine induced cAMP/PKA-dependent inhibition of ASIC channel currents through opioid receptors. Additionally, Endres-Becker et al. (2007) reported the μ -opioid-mediated inhibition of the TRPV1 channel via Gi/o proteins and the cAMP pathway. In this manner, we sought to verify whether the interaction between LQFM-096 and these channels is through activation of the opioid pathway. In the acidic saline- and capsaicin-induced nociception, naloxone blocked the antinociceptive effects of LQFM-096. This result suggests that the inhibition of these channels by LQFM-096 is dependent on the opioid pathway.

The development of mechanical hyperalgesia has been associated with the TRPV1 ion channels and ASICs (Watanabe et al. 2015; White et al. 2010). The antihyperalgesic

effects of LQFM-096 suggest that inhibition of these channels is involved in the activation of the opioid pathway.

Despite the potential roles of ion channels and the opioid pathway in the antinociceptive activity of LQFM-096, non-blockade of the second phase of the formalin test by antagonists suggest that the analgesic effects of this compound involve an anti-inflammatory component. According to Giorno et al. (2016), the antinociceptive effect in the first phase is associated with a direct action on the opioid pathway while the antinociceptive effect in the second phase involves the inhibition of inflammatory mediators.

The anti-inflammatory actions of LQFM-096 were investigated through carrageenan-induced paw oedema and pleurisy. Carrageenan induces inflammation by releasing mediators such as histamine, serotonin, bradykinin, prostaglandins and nitric oxide (Di Rosa 1972; Passos et al. 2007). In these tests, LQFM-096 elicited anti-inflammatory activities by reducing the recruitment of polymorphonuclear cells (such as neutrophils) and suppressing oedema formation.

Neutrophil granules are rich in MPO. This enzyme often interacts with hydrogen peroxide and chloride to generate hypochlorous acid inside the phagosome, thus eliminating the aggressor agent (Klebanoff 2005). LQFM-096 reduced the MPO activity. This result corroborates the reduction in polymorphonuclear cells in the previous study (Haegens et al. 2009).

The involvement of TNF- α in the anti-inflammatory actions of LQFM-096 was also assessed. TNF- α is a potent inflammatory mediator that regulates the induction of adhesion molecules in the endothelium and contribute to the recruitment of leukocytes to inflammatory sites (Nourshargh and Alon 2014; Zelová and Hosek 2013). In this study, LQFM-096 reduced TNF- α levels. This effect appears to contribute to the reduction in cell migration, MPO activity, and subsequent anti-inflammatory activity.

Furthermore, in this study, it was observed that LQFM-096 reduced the PGE₂ levels in the pleural exudate, corroborating with result obtained in the PGE₂-induced hyperalgesia. Therefore, part of the anti-inflammatory effect of LQFM-096 involves the inhibition of PGE₂ production.

In the presence of pro-inflammatory mediators, the expression of ASICs and TRPV1 channels is increased. This increase, in turn, could facilitate the development and maintenance of inflammatory pain (Ma and Quirion 2007; White et al. 2010). Therefore, the anti-inflammatory activity of this compound may decrease the expression and activation of these channels. Hypothetically, the antinociceptive effects of LQFM-096 could be considered to be independent of the opioid pathway if the latter assumption is true. This hypothesis seems to be supported by the non-blockade effect of LQFM-096 in the second phase of the formalin test.

Finally, we investigated the effects of LQFM-096 on CFA-induced arthritis, which is a chronic inflammatory

model. This is a well-established model for the evaluation of substances with anti-arthritic potential, as it mimics arthritis in clinical setup (Vijayalaxmi et al. 2015). This model is associated with oedema formation and a reduction in the nociceptive threshold (Raj Kapoor et al. 2009). Although treatment with LQFM-096 did not reduce the formation of oedema, attenuation of hyperalgesia and a reduction in polymorphonuclear cell infiltration in the paw dermis were reported. These results showed that the anti-inflammatory effects of LQFM-096 were maintained in the chronic model.

Conclusions

This study showed that oral administration of LQFM-096 exerts acute antinociceptive effects. The attenuation of the analgesic effects of this compound by pretreatment with naloxone and glibenclamide suggest that the antinociceptive activity of this triazole derivative is likely mediated by the activation of opioid receptors and K_{ATP} channels as well as opioid-dependent inhibition of ASICs and TRPV1 ion channels. The LQFM-096-induced anti-inflammatory effect involves reduction in TNF- α and PGE₂ levels, cell migration and MPO activity in animal models of inflammation. Altogether, these findings suggest that LQFM-096 might be a promising prototype for developing a new analgesic and anti-inflammatory agents.

Acknowledgments The authors are grateful to Dr. Ekaterina A. F. B. Rivera, Lucas B. do Nascimento and Taís Andrade Dias de Souza for ethical and technical assistance, as well as the CNPq (Conselho Nacional de Desenvolvimento Científico e Tecnológico), and CAPES (Coordenação de Aperfeiçoamento de Pessoal de Nível Superior) for financial support.

Compliance with ethical standards

Conflict of interest The authors declare no conflicts of interest.

References

- Alterman M, Hallberg A (2000) Fast microwave-assisted preparation of aryl and vinyl nitriles and the corresponding tetrazoles from organo-halides. *J Org Chem* 65(23):7984–7989. <https://doi.org/10.1021/jo0009954>
- Anseloni VCZ, Ennis M, Lidow MS (2003) Optimization of the mechanical nociceptive threshold testing with the Randall-Selitto assay. *J Neurosci Met* 13:93–97. [https://doi.org/10.1016/S0165-0270\(03\)00241-3](https://doi.org/10.1016/S0165-0270(03)00241-3)
- Baggio CH, Freitas CS, Marcon R, Werner MF, Rae GA et al (2012) Antinociception of b-d-glucan from *Pleurotus pulmonarius* is possible related to protein kinase inhibition. *Int Biol Macromol* 50:872–877
- Barbosa FL, Mori LS, Riva D, Stefanello MÉ, Zamprônio AR (2013) Antinociceptive and anti-inflammatory activities of the ethanolic extract, fractions and 8-methoxylapachenol from *Sinningia allagophylla* tubers. *Basic Clin Pharmacol Toxicol* 113:1–7
- Benyamin R, Trescot AM, Datta S, Buenaventura R, Adlaka R et al (2008) Opioid complications and side effects. *Pain Physician* 11:S105–S120
- Cai Q, Qiu C, Qiu F, Liu T, Qu Z et al (2014) Morphine inhibits acid-sensing ion channel currents in rat dorsal root ganglion neurons. *Brain Res* 1554:12–20. <https://doi.org/10.1016/j.brainres.2014.01.042>
- Campbell VC, Welch SP (2001) The role of minoxidil on endogenous opioid peptides in the spinal cord: a putative co-agonist relationship between K-ATP openers and opioids. *Eur J Pharmacol* 417(1–2):91–98
- Chandy RL, Moore PK (1998) Effects of selective inhibitors of neuronal nitric oxide synthase on carrageenan-induced mechanical and thermal hyperalgesia. *Neuropharmacology* 37(1):37–43
- Chopade AR, Sayyad FJ (2013) Antinociceptive effect of *Phyllanthus fraternus* extract in complete Freund's adjuvant induced chronic pain in mice. *Biomed Aging Pathol* 3:235–240
- Costa EA, Lino RC, Gomes MN, Nascimento MNM, Florentino IF et al (2013) Anti-inflammatory and antinociceptive activities of LQFM 002—a 4-nerolidylcatechol derivative. *Life Sci* 92:237–244. <https://doi.org/10.1016/j.lfs.2012.12.003>
- Deval E, Lingueglia E (2015) Acid-sensing ion channels and nociception in the peripheral and central nervous systems. *Neuropharmacology* 94:49–57. <https://doi.org/10.1016/j.neuropharm.2015.02.009>
- Deval E, Gasull X, Noël J, Salinas M, Baron A et al (2010) Acid-sensing ion channels (ASICs): pharmacology and implication in pain. *Pharmacol Ther* 128:549–558. <https://doi.org/10.1016/j.pharmthera.2010.08.006>
- Dheer D, Singh V, Shankar R (2017) Medicinal attributes of 1,2,3-triazoles: current developments. *Bioorg Chem* 71:30–54
- Di Rosa M (1972) Biological properties of carrageenan. *J Pharmacol* 24(2):89–102
- Endres-Becker J, Heppenstall PA, Mousa SA, Labuz D, Oksche A et al (2007) Mu-opioid receptor activation modulates transient receptor potential vanilloid 1 (TRPV1) currents in sensory neurons in a model of inflammatory pain. *Mol Pharmacol* 71:12–18. <https://doi.org/10.1124/mol.106.026740>
- Fein A (2011) Nociceptores: as células que sentem dor. Tradução de PETROV, P.; FRANCISCHI, J. N.; FERREIRA, S. H. Ribeirão Preto/SP. 2011. Disponível em: http://cell.uchc.edu/pdf/fein/nociceptores_fein_2012.pdf
- Florentino IF, Silva DPB, Silva DM, Cardoso CS, Moreira ALE, Borges CL, Soares CMA, Galdino PM, Lião LM, Ghedini PC, Menegatti R, Costa EA (2017) Potential anti-inflammatory effect of LQFM-021 in carrageenan-induced inflammation: the role of nitric oxide. *Nitric Oxide* 69:35–44. <https://doi.org/10.1016/j.niox.2017.04.006>
- Giorno TBS, Da Silva BV, Pinto AC, Fernandes PD (2016) Antinociceptive effect and mechanism of action of isatin, N-methyl isatin and oxopropyl isatin in mice. *Life Sci* 15:189–198
- Gold MS, Gebhart GF (2010) Nociceptor sensitization in pain pathogenesis. *Nat Med* 16(11):1248–1257. <https://doi.org/10.1038/nm.2235>
- Gregory N, Harris AL, Robinson CR, Dougherty PM, Fuchs PN, Sluka KA (2013) An overview of animal models of pain: disease models and outcome measures. *J Pain* 14(11):1255–1269
- Gupta D, Jain DK (2017) Synthesis, antifungal and antibacterial activity of novel 1,2,4-triazole derivatives. *J Adv Pharm Technol Res.* 6:141–146. <https://doi.org/10.4103/2231-4040.161515>
- Haegens A, Heeringa P, Suylen RJV, Steele C, Aratani Y et al (2009) Myeloperoxidase deficiency attenuates Lipopolysaccharide-induced acute lung inflammation and subsequent cytokine and chemokine production. *J Immunol* 182(12):7990–7996

- Hagmann WK (2008) The many roles for fluorine in medicinal chemistry. *J Med Chem* 51:4359–4369. <https://doi.org/10.1021/jm800219f>
- Hanskaar S, Hole K (1987) The formalin test in mice: dissociation between inflammatory and non-inflammatory pain. *J Pain* 30(1):103–114. [https://doi.org/10.1016/0304-3959\(87\)90088-1](https://doi.org/10.1016/0304-3959(87)90088-1) <http://www.iasp-pain.org/Taxonomy>. Pain terms, a current list with definitions and notes on usage (pp 209–214). Classification of Chronic Pain, Second Edition, IASP Task Force on Taxonomy, edited by H. Merskey and N. Bogduk, IASP Press, Seattle, ©1994
- Hunashal RD, Ronad PM, Maddi VS, Satyanarayana D, Kamadod MA (2014) Synthesis, anti-inflammatory and analgesic activity of 2-[4-(substituted benzylideneamino)-5-(substituted phenoxyethyl)-4H-1,2,4-triazol-3-ylthio] acetic acid derivatives. *Arab J Chem* 7(6):1070–1078. <https://doi.org/10.1016/j.arabjc.2011.01.003>
- Jage J (2005) Opioid tolerance and dependence. Do they matter?. *Eur J Pain* 9:157–162. <https://doi.org/10.1016/j.ejpain.2004.11.009>
- Ji RR, Xu ZZ, Gao YJ (2014) Emerging targets in neuroinflammation-driven chronic pain. *Nat Rev Drug Discov* 13:533–538. <https://doi.org/10.1038/nrd4334>
- Joanna L, Talarek S, Orzelska J, Fidecka S, Wujec M, Plech T (2014) The antinociceptive effect of 4-substituted derivatives of 5-(4-chlorophenyl)-2-(morpholin-4-ylmethyl)-2,4-dihydro-3H-1,2,4-triazole-3-thione in mice. *Naunyn-Schmiedeberg's Arch Pharmacol* 387:367–375. <https://doi.org/10.1007/s00210-013-0938-0>
- Julius D, Basbaum AI (2001) Molecular mechanisms of nociception. *Nature* 413:203–210. <https://doi.org/10.1038/35093019>
- Kawabata A (2001) Prostaglandin E2 and pain—an update. *Biol Pharm Bull* 34(8):1170–1173
- Khanage SG, Raju A, Mohite PB, Pandhare RB (2013) Analgesic activity of some 1,2,4-triazole heterocycles clubbed with pyrazole, tetrazole, isoxazole and pyrimidine. *Adv Pharm Bull* 3(1):13–18. <https://doi.org/10.5681/apb.2013.003>
- Klebanoff SJ (2005) Myeloperoxidase: a friend and foe. *J Leuk Biol* 77:598–625
- Koster R, Anderson M, De Beer EJ (1959) Acetic acid for analgesic screening. *Fed Proc* 18:412
- L'abbé G, Bruynseels M, Delbeke P, Topper S (1990) Molecular rearrangements of 4-iminomethyl-1,2,3-triazoles replacement of 1-aryl substituents in 1H-1,2,3-triazoles-4-carbaldehydes. *J Heterocycl Chem* 27:2021
- Li J, Zhang J, Rodrigues MC, Ding D, Longo JPF et al (2016) Synthesis and evaluation of novel 1,2,3-triazole-based acetylcholinesterase inhibitors with neuroprotective activity. *Bioorg Med Chem Lett* 26(16):3881–3885. <https://doi.org/10.1016/j.bmcl.2016.07.017>
- Lima LM, Barreiro EJ (2005) Bioisosterism: a useful strategy for molecular modification and drug design. *Curr Med Chem* 12:23–49
- Ma W, Quirion R (2007) Inflammatory mediators modulating the transient receptor potential vanilloid 1 receptor: therapeutic targets to treat inflammatory and neuropathic pain. *Expert Opin Ther Targets* 11(3):307–320
- Meotti FC, Coelho IS, Santos ARS (2010) The nociception induced by glutamate in mice is potentiated by protons released into solution. *J Pain* 11(6):570–578. <https://doi.org/10.1016/j.jpain.2009.09.012>
- Mickle AD, Shepherd AJ, Mohapatra DP (2016) Nociceptive TRP channels: sensory detectors and transducers in multiple pain pathologies. *J Pharm* 9:72. <https://doi.org/10.3390/ph9040072>
- Mohd Sani MH, Zakaria ZA, Balan T, The LK, Salleh MZ (2012) Antinociceptive activity of methanol extract of *Muntingia calabura* leaves and the mechanisms of action involved. *J Evid Based Complement Altern Med* 2012:1–10. <https://doi.org/10.1155/2012/890361>
- Montes GC, Silva BNM, Rezende B, Sudo RT, Ferreira VF (2017) The hypnotic, anxiolytic, and antinociceptive profile of a novel μ -opioid agonist. *Molecules* 22:800. <https://doi.org/10.3390/molecules22050800>
- Moore AR (2003) Pleural models of inflammation: immune and non-immune. In: Winyard PG, Willoughby DA (eds) *Inflammation protocols*. Humana Press, Totowa, pp 123–128
- Nourshargh S, Alon R (2014) Leukocyte migration into inflamed tissues. *Immunity*. <https://doi.org/10.1016/j.immuni.2014.10.008>
- Oliveira LP, Silva DPB, Florentino IF, Fajemiroye JO, Oliveira TS et al (2016) New pyrazole derivative 5-[1-(4-fluorophenyl)-1H-pyrazol-4-yl]-2H-tetrazole: synthesis and assessment of some biological activities. *Chem Biol Drug Des*. <https://doi.org/10.1111/cbdd.12838>
- Oliveira-Junior JO, Portela Junior CSA, Cohen CP (2016) Inflammatory mediators of neuropathic pain. *Sociedade Brasileira para o Estudo da Dor* 17(Suppl 1):S35–S42. <https://doi.org/10.5935/1806-0013.20160045>
- Passos GF, Fernandes ES, da Cunha FM, Ferreira J, Pianowski LF et al (2007) Anti-inflammatory and anti-allergic properties of the essential oil and active compounds from *Cordia verbenacea*. *J Ethnopharmacol* 110(2):323–333
- Peng Y, Zhang Q, Arora S, Keenan SM, Kortagere S et al (2009) Novel delta opioid receptor agonists exhibit differential stimulation of signaling pathways. *Bioorg Med Chem* 17:6442–6450. <https://doi.org/10.1016/j.bmc.2009.07.007>
- Penthala NR, Madhukuri L, Thakkar S, Madadi NR, Lamture G et al (2015) Synthesis and anti-cancer screening of novel heterocyclic-1,2,3-triazoles as potential anticancer agents. *Med Chem Commun J* 6:1535–1543. <https://doi.org/10.1039/C5MD00219B>
- Porreca F, Ossipov MH (2009) Nausea and vomiting side effects with opioid analgesics during treatment of chronic pain: mechanisms, implications, and management options. *Pain Med* 10(4):654–662. <https://doi.org/10.1111/j.1526-4637.2009.00583.x>
- Portman R (1998) WO Patent 9802423
- Rajk Kapoor B, Kavimani S, Ravichandiran V, Sekhar K, Senthil Kumar R et al (2009) Effect of *Indigofera aspalathoides* on complete Freund's adjuvant-induced arthritis in rats. *Pharm Biol* 47(6):553–557. <https://doi.org/10.1080/13880200902902489>
- Randall LO, Selitto JJ (1957) A method for measurement of analgesic activity on inflamed tissue. *Arch Int Pharmacodyn Thé* 4:409–419
- Rios ERV, Rocha NFM, Carvalho AMR, Vanconcelos LF, Dias ML et al (2013) TRP and ASIC channels mediate the antinociceptive effect of citronellyl acetate. *Chem Biol Interact* 203:573–579. <https://doi.org/10.1016/j.cbi.2013.03.014>
- Roschangar F, Sheldon RA, Senanayake CH (2015) Overcoming barriers to green chemistry in the pharmaceutical industry—the Green Aspiration Level™ concept. *Green Chem* 17:752–758. <https://doi.org/10.1039/c4gc01563k>
- Sakurada T, Katsumata K, Tan-No K, Sakurada S, Kisara K (1992) The capsaicin test in mice for evaluating tachykinin antagonists in the spinal cord. *Neuropharmacol J* 31:1279–1285
- Saleh TSF, Calixto JB, Medeiros YS (1999) Effects of anti-inflammatory drugs upon nitrate and myeloperoxidase levels in the mouse pleurisy induced by carrageenan. *Peptides* 20(8):949–956
- Sedgwick AD (1995) Initiation of inflammatory response and its prevention. In: Bonta IL, Bray MA (eds) *EUA: handbook of inflammation*. Elsevier, New York, p 253
- Sehgal N, Smith H, Manchikanti L (2011) Peripherally acting opioids and clinical implications for pain control. *Pain Physician* 14:249–258
- Shibata M, Ohkubo T, Takahashi H, Inoki R (1989) Modified formalin test: characteristic biphasic pain response. *Pain* 38(3):347–352
- Sokal RR, Rohlf FJ (1981) *Biometry: the principles and practice of statistics in biological research*. W.H. Freeman and Co., New York

- Trost BM (1991) The atom economy—a search for synthetic efficiency. *Science* 254:1471
- Tsuchida K, Ibuki T, Matsumura K (2015) Bromoenol lactone, an inhibitor of calcium-independent phospholipase A2, suppresses carrageenan-induced prostaglandin production and hyperalgesia in rat hind paw. *Mediators Inflamm* 2015:1–7. <https://doi.org/10.1155/2015/605727>
- Vijayalaxmi A, Bakshi V, Begum N, Kowmudi V, Naveen Kumar NY, Reddy Y (2015) Anti-arthritic and anti-inflammatory activity of beta caryophyllene against Freund's complete adjuvant induced arthritis in wistar rats. *Bone Rep Recomm* 1:29. <https://doi.org/10.4172/2469-6684.10009>
- Wang J, Sánchez-Roselló M, Aceña JL, del Pozo C, Sorochinsky AE et al (2014) Fluorine in pharmaceutical industry: fluorine-containing drugs introduced to the market in the last decade (2001–2011). *Chem Rev* 114:2432–2506. <https://doi.org/10.1021/cr4002879>
- Watanabe M, Ueda T, Shibata Y, Kumamoto N, Ugawa S (2015) The role of TRPV1 channels in carrageenan-induced mechanical hyperalgesia in mice. *NeuroReport* 26(3):173–178
- Wemmie JA, Taugher RJ, Kreple CJ (2013) Acid-sensing ion channels in pain and disease. *Nat Rev Neurosci* 14(7):461–471. <https://doi.org/10.1038/nrn3529>
- White JPM, Cibelli M, Fidalgo AR (2010) Role of transient receptor potential and acid-sensing ion channels in peripheral inflammatory pain. *Anesthesiology* 112:729–741
- Yet L (2018) Privileged structures in drug discovery medicinal chemistry and synthesis, 1st edn. Wiley, Hoboken
- Zelová H, Hosek J (2013) TNF- α signalling and inflammation: interactions between old acquaintances. *Inflamm Res* 62:641–651. <https://doi.org/10.1007/s00011-013-0633-0>
- Zwaagstra ME, Timmerman H, Tamura M, Tohma T, Wada Y et al (1997) Synthesis and structure-activity relationships of carboxylated chalcones: a novel series of CysLT1 (LTD4) receptor antagonists. *J Med Chem* 40(7):1075–1089. <https://doi.org/10.1021/jm960628d>

Publisher's Note Springer Nature remains neutral with regard to jurisdictional claims in published maps and institutional affiliations.